CORTEX 187 (2025) 124–139

Available online at www.sciencedirect.com

ScienceDirect

Journal homepage: www.elsevier.com/locate/cortex

Research Report

Impaired rapid neural face categorization after reversing long-lasting congenital blindness

José P. Ossandón [a,*], Bruno Rossion [b,c], Giulia Dormal [a], Ramesh Kekunnaya [d] and Brigitte Röder [a,d]

[a] Biological Psychology and Neuropsychology, Hamburg University, Hamburg, Germany
[b] Université de Lorraine, CNRS, IMoPA, Nancy, France
[c] Université de Lorraine, CHRU-Nancy, Service de Neurologie, Nancy, France
[d] Child Sight Institute, Jasti V Ramanamma Children's Eye Care Center, LV Prasad Eye Institute, Hyderabad, India

ARTICLE INFO

Article history:
Received 21 January 2025
Revised 13 April 2025
Accepted 14 April 2025
Action editor Jeremy Tree
Published online 26 April 2025

Keywords:
Congenital cataract
Sight-restoration
Face categorization
Sensitive period
EEG FPVS

ABSTRACT

Transient early visual deprivation in humans impairs the processing of faces more than of other object categories. While configural face processing and face individuation appear to be largely impaired in sight recovery individuals following congenital visual deprivation, their behavioral ability to categorize stimuli as faces has been described as preserved. Here we thoroughly investigated rapid automatic face categorization in individuals who had recovered sight after congenital blindness. Eighteen participants (6 women, 12 men) who had undergone congenital cataract reversal surgery participated in a well-validated electroencephalographic (EEG) experiment with fast periodic visual stimulation (FPVS) to elicit automatic neural face-categorization responses from variable natural images. As normally sighted controls ($N = 13$) and individuals with reversed developmental cataracts ($N = 16$), congenital cataract reversal individuals exhibited clear neural face-categorization activity. However, their neural face categorization responses were significantly weaker and delayed. These observations show that previous behavioral studies with explicit tasks lacked sensitivity to uncover altered face categorization in sight-recovery individuals with a history of congenital cataracts. This indicates that early experience is necessary for categorization too. We speculate that altered neural correlates of face categorization result from a lower selectivity of face-selective areas of the ventral occipito-temporal cortex, impeding higher-order face processes such as face identity recognition.

© 2025 The Author(s). Published by Elsevier Ltd. This is an open access article under the CC BY license (http://creativecommons.org/licenses/by/4.0/).

* *Corresponding author.*
E-mail address: jose.ossandon@uni-hamburg.de (J.P. Ossandón).
https://doi.org/10.1016/j.cortex.2025.04.007
0010-9452/© 2025 The Author(s). Published by Elsevier Ltd. This is an open access article under the CC BY license (http://creativecommons.org/licenses/by/4.0/).

1. Introduction

Deprivation of patterned visual experience during infancy, such as in cases of congenital cataract, can lead to lifelong difficulties in face identity recognition. Even with early sight-restoring treatment, as before six months of age, individuals might still grow to experience deficits in face memory and in discriminating between faces that vary on feature spacing, point of view, or lighting (de Heering & Maurer, 2014; Geldart et al., 2002; Le Grand et al., 2001; Putzar et al., 2010; Robbins et al., 2010). Such deficits indicate that visual experience during sensitive periods is crucial for the development of cortical circuits involved in face recognition (Maurer et al., 2005; Röder & Kekunnaya, 2022).

Accordingly, changes in the neural circuits involved in face processing have been demonstrated in functional magnetic resonance (fMRI) and electroencephalographic (EEG) studies with individuals who recovered sight after short (Grady et al., 2014) and prolonged visual deprivation (Röder et al., 2013), respectively. For instance, in an event-related potential (ERP) study, sight-recovery individuals with prolonged durations of congenital blindness did not exhibit the typical enhancement of the N170 when viewing face stimuli (Röder et al., 2013), that is, the earliest and most consistent ERP typically associated with face-selectivity (Bentin et al., 1996). Most recently, an fMRI study in congenital cataract-reversal individuals showed dramatically reduced face-selectivity in the cortical regions of the ventral occipito-temporal cortex (VOTC) that, in humans with normal visual development, respond more strongly to faces than other visual categories (Rączy et al., 2024). Crucially, the same sight-recovery individuals did develop neural selectivity for other visual categories like scenes and body parts, suggesting a unique impact of early visual deprivation on face processing (Rączy et al., 2024). However, despite these observations, and in contrast to deficits in recognizing the identity of faces, individuals treated for congenital cataracts seem to have little difficulty with face categorization, meaning that they are able to behaviorally differentiate faces from non-faces (Mondloch et al., 2003, 2013), even if the visual deprivation lasted for years rather than weeks or months (Gandhi et al., 2017; Ostrovsky et al., 2006; Röder et al., 2013).

Considering this discrepancy and to clarify the role of early visual experience in face categorization, here we thoroughly assessed face categorization in individuals treated for congenital cataracts. We measured a valid and robust neural face categorization response in a normally sighted group and contrasted it to the response observed in sight-recovery individuals who had experienced long-term visual deprivation due to congenital cataracts. More specifically, we employed a frequency-tagging approach in which variable natural images of faces appear at a fixed rate (one every five) within a rapid (6 Hz) periodic stream of variable non-face natural stimuli (Rossion et al., 2015) (see Fig. 1). While the common neural response to faces and non-face stimuli is recorded at 6 Hz, a direct measure of face-selectivity (i.e., reliable differences between faces and other stimuli) can be objectively identified and quantified at the face frequency of interest (6 Hz/5 = 1.2 Hz) and its harmonics. This approach implicitly measures face categorization and as has been validated in more than 40 studies with a variety of and populations (human adults, children and infants; non-human primates) and methods (EEG: Rossion et al., 2015; MEG: Hauk et al., 2021; intracranial EEG: Jonas et al., 2016; fMRI: Gao et al., 2018). Frequency tacking is highly sensitive and typically provides robust face-selective neural responses in a few minutes, and, importantly for the present study, directly relates to behavioral face categorization ability (Retter et al., 2020). In addition, since stimuli are presented at a rapid rate, the frequency tacking approach is particularly suited for use in individuals with reversed congenital cataracts who suffer from gaze instability (nystagmus). We hypothesized that patients with reversed congenital cataracts show impaired rapid and automatic face categorization

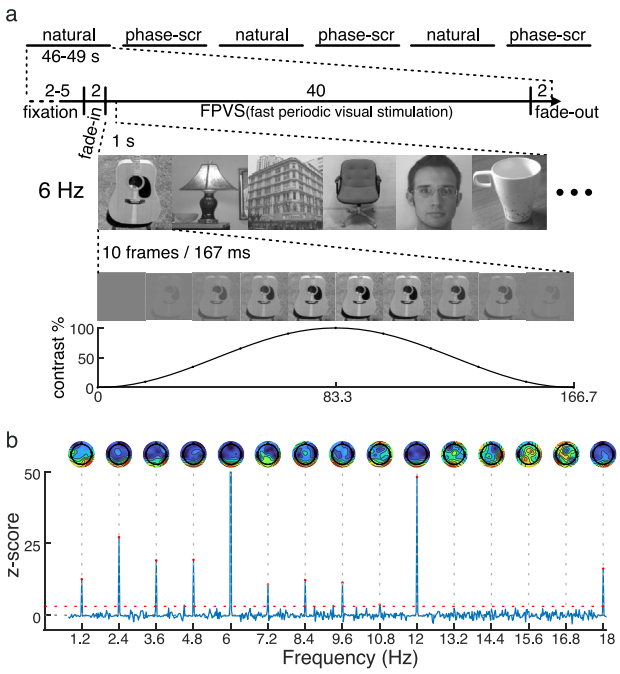

Fig. 1 – Experimental procedure and selection of harmonics. (a) The experiment consisted of six FPVS sequences: three with natural images and three with phase-scrambled images. During each stimulation period, images were presented at a *Base rate* of 6 Hz through sinusoidal contrast modulation. Every 5th image (1.2 Hz, *Face rate*) was a face varying in identity, size, and viewpoint. Prior to the main experiment, 11 out of 18 CC individuals completed a brief face categorization test; all of them achieved an accuracy of 100% (see Suppl. Fig. 1 to see the full test material) (b) Z-score values for different frequency bins, calculated from the grand-average amplitude spectrum across all participants and occipitoparietal channels. Harmonics of the Base and at the Face rate were selected for further analysis if their z-score exceeded 3.09 (indicated by the horizontal red dotted line, $p = .001$). The corresponding scalp topographies are displayed above each harmonic frequency.

compared to individuals with reversed developmental cataracts and normally sighted controls.

2. Materials and methods

2.1. Participants

The sample size was determined by participant availability within the project's duration, targeting a range of 10–20 participants as in previous studies using the same experimental paradigm (e.g., Jacques et al., 2016; Quek et al., 2018; Retter et al., 2020; Rossion et al., 2015). Three different groups were recruited at the LV Prasad Eye Institute and the local community of Hyderabad (India) for this study:

(1) Congenital cataract reversal group (CC): This group included individuals with a clinical history of dense bilateral congenital cataracts and related patterned visual deprivation from birth. Evidence for the absence of patterned vision before cataract surgery was established through the morphology of cataract a lack of fundus view and retinal glow prior to surgery. Additional criteria for classification included nystagmus, sensory strabismus, positive family history, and absorbed cataractous lens status.

The CC group comprised 18 sight-recovery participants (6 women, 12 men; mean age: 20.4 years; range: 8–41; see Table 1 for a detailed description of all participants). They had their cataracts removed at a mean age of 10.1 years and were tested on average 10.3 years post-surgery (range: 6 months–35.4 years). Thirteen participants had implanted intraocular lenses, while the remaining used corrective glasses. Six CC individuals presented eyes with absorbed cataracts that regularly emerge after some years without treatment in congenital cases. Absorbed cataract is easy to distinguish from partial cataracts by their morphology. From the 13 individuals who had a visual acuity assessment before surgery, 12 fell under the WHO's category of blind (i.e., had a visual acuity of less than 3/60) (World Health Organization, 2019). The remaining CC individual had a severe visual impairment (logMar visual acuity = 1) which was related to the patient's absorbed cataractous lens. All CC participants had nystagmus, indicating the absence of pattern vision in the first weeks after birth (Abadi et al., 2006; Gelbart et al., 1982; Lambert et al., 2006). Their average post-surgical logMar visual acuity was .89 (range: .3–1.3).

Table 1 – Participants description.

	Age at testing (years)	Age at surgery (years)	Cataract type at surgery	Presurgical visual acuity (best eye)	Last visual acuity (CC/DC: postsurgical) (best eye)		Cataract Family history	Strabismus	Face-object test
					Decimal	logMAR			
Congenital cataract group (CC, $N = 18$)									
cc-1	26.2	.5	Dense	Unknow	.16	.8	–	Eso.	Yes
cc-2	37.7	2.2	Dense	Unknow	.5	.3	+	Eso.	No
cc-3	13.5	7.0	Absorbed	CF 3 m	.16	.8	–	No	Yes
cc-4	33.7	6.0	Dense	Unknow	.05	1.3	+	Unkn.	No
cc-5	9.9	6.2	Absorbed	.016	.1	1	+	Yes	No
cc-6	31.5	17.6	Dense	CF CF	.06	1.2	Unkn.	Yes	Yes
cc-7	31.3	13.6	Dense	Unknow	.1	1	+	Eso.	Yes
cc-8	17.3	16.4	Absorbed	.06	.16	.8	+	No	Yes
cc-9	16.3	15.4	Absorbed	.03	.08	1.1	+	Eso.	Yes
cc-10	41.7	20.7	Absorbed	.1	.1	1	+	Yes	Yes
cc-11	16.0	15.6	Absorbed	.03	.1	1.1	–	Exo.	Yes
cc-12	12.7	11.5	Dense	CF CF	.06	1.2	+	No	Yes
cc-13	8.8	5.7	Dense	Unknow	.16	.8	Unkn.	Yes	No
cc-14	9.8	4.0	Dense	PL+, PR	.1	1	+	No	No
cc-15	21.8	17.8	Dense	CF .5 m	.2	.7	+	Eso.	No
cc-16	12.5	1.0	Dense	FFL	.2	.7	–	Eso.	Yes
cc-17	16.8	15.8	Dense	CF .5 m	.15	.8	Unkn.	Eso.	No
cc-18	10.0	5.4	Dense	FFL	.31	.5	Unkn.	Eso.	Yes
Summary	M: 20.4 R: 8–41	M: 10.1 R: .5–20.7			GM: .13	M: .89			
Developmental cataract control group (DC, $N = 16$)									
Summary	M: 14.9 R: 9.2–24.6	M: 8.8 R: 2.5–14.2	5 dense		GM: .68 R: .33–1	M: .17 R: 0–.48	2 + 2 unkn.	2 Exo.	
Normally sighted control group (MCC, $N = 13$)									
Summary	M: 22.6 R: 9.5–42.5				1.4	M:-.145 R: –.29 – .25			

PL: perception light; PR: projection of rays; CF: counting finger, equivalence with logMAR acuity has been reported to be 1.7–2.0 with CF at 30 cm (Schulze-Bonsel et al., 2006); CF CF: counting finger close to face; FFL: fixate and follows light; HM: hand movement; M: mean; GM: geometric mean; R: range; Exo: exotropia; Eso: esotropia. Categories of visual impairment in terms of visual acuity are defined as: mild/worse than .5 decimal units, moderate/worse than .33, severe/worse than .1, and blindness/worse than .05 (World Health Organization, 2019).

(2) Matched normally sighted control group (MCC): This group comprised 13 individuals (3 women, 10 men, mean age: 22.6 years, range: 9.5–42.5) with normal visual development and normal or corrected-to-normal vision. Their average logMar visual acuity was −.145 (range: −.29 − .25). This group was age-matched to the CC group, with no significant age difference at testing [$t_{(29)=}$- .5, $p = .5$].
(3) Developmental cataract reversal group (DC): This control group comprised 16 individuals (6 women, 10 men, mean age: 14.9 years, range: 9.2–24.6) with a transient phase of bilateral cataracts, which had not necessarily been dense or total. They underwent cataract removal surgery at a mean age of 8.8 years (range: 2.5–14.2) and were tested on average 6.1 years post-surgery (range: 7 months–22.1 years). Their average post-surgical logMar visual acuity was .17 (range: 0–.48). Expect one, none of the DC participants presented with nystagmus. All DC participants were fitted with intraocular lenses.

All individuals were tested at the LV Prasad Eye Institute in Hyderabad, India. None had any other known sensory system deficit or neurological disorder. Expenses for participation were reimbursed, and minors received a small present. Participants, and when applicable, their legal guardians, were informed about the study in a language they understood (in most cases Hindi, Telugu or English) and provided written informed consent before participating. The study was approved by the ethics boards of the Faculty of Psychology and Human Movement at the University of Hamburg, Germany, and the LV Prasad Eye Institute.

2.2. Stimuli

The employed stimulus set, previously used in several studies (e.g., Jonas et al., 2016; Rossion et al., 2015), consisted of 254 non-face "natural" images (objects, animals, plants and buildings) and 51 face images (the complete set of images is available at https://face-categorization-lab.webnode.com/resources/natural-face-stimuli/). The images were grayscale and equalized in terms of luminance and contrast. Importantly, the images were unsegmented close-ups that varied in size, viewpoint, and background. From each image, a control "phase-scrambled" version was created by scrambling its phase in the 2-D spatial frequency domain. These phase-scrambled images were used to ensure that any observed face-selected signal was not due to differences in low-level properties between image categories, specifically those that are dependent on the distribution of power in the spatial spectral domain (Rossion et al., 2015). Stimuli were displayed at 80 cm in the center of the screen with a resolution of 200 × 200 pixels, subtending 10 × 10 visual degrees. Stimuli were presented on a Dell LCD monitor (IN2030M) with a resolution of 1600 × 900 at a refresh rate of 60 Hz.

2.3. Face versus object discrimination test

Eleven of the eighteen CC participants were assessed with a short non-standardized custom face-screening test which aimed at identifying major deficits in the ability to discriminate faces from non-face stimuli. Normally sighted controls perform in this screening at 100%. The test included 6 full-screens PowerPoint slides (see Suppl. Fig. 1). Four of the slides displayed a single large photo: a frontal view of a face (one grayscale image of a man and one color image of a woman) or a central object (one house and one flower, both grayscale). Participants were asked to identify what was presented on each slide. The remaining two slides each showed six grayscale images of the same size arranged in 2 rows and 3 columns. One of these images was a face, which participants had to point out. All CC individuals who took this test responded correctly in 100% of the trials and spontaneously provided the correct gender of the face stimuli too.

2.4. Procedure

Participants watched sequences of stimuli presented at 6 Hz for 44 sec (see Fig. 1a). The sequence was contrast-modulated following a sinusoidal function. Each stimulus cycle lasted ~166 msec (1000 msec/6), starting by increasing its contrasts from the uniform gray background, reaching full contrast at half the cycle, and then decreasing the contrast again to complete the cycle. Every fifth stimulus was a face image. Therefore, although the overall sequence of images, including objects and faces, was presented at 6 Hz ("Base rate"), faces were specifically presented at a rate of 1.2 Hz (6 Hz/5, "Face rate"). This design ensures that a distinguishable EEG signal at the Face rate or any of its harmonics (2.4 Hz, 3.6 Hz, etc.) would appear only under specific circumstances: First, participants must be able to discriminate between faces and objects during the rapid presentation of stimuli. Second, to generate a periodical face-selective signal, they must be able to perform this discrimination across faces displayed in different sizes, different viewpoints, lighting directions, etc. Notably, this FPVS approach provides a genuine neural face categorization signal without signal subtraction, commonly used when stimuli are presented at non-periodic rates with long and (usually) temporally jittered intervals (Rossion et al., 2018).

The experiment consisted of six stimulation sequences: three with sequences of natural stimuli and three with phase-scrambled stimuli. Each sequence began with a 2 to 5-s period of a blank screen with a fixation cross in the middle. The fixation cross subtended an angle of .8° when viewed from 80 cm and remained visible throughout the entire sequence. Next the flickering stimuli were presented. The first images gradually faded in over 2 sec, with the maximum contrast increasing steadily from 0 to 100%. The next images were presented up to 100% contrast at a stimulation rate of 6 Hz for 40 sec. The sequence ended with the last images gradually fading out over a 2-s period (from 100% to 0% contrast). To ensure that participants remained attentive, they were instructed to press the number 7 key to the keyboard's number pad whenever they noticed a change in the color of the fixation cross. The fixation cross changed from black to red for 500 msec, occurring 10 times per sequence. Participants who were too young or unable to press the key were asked to tap the table with their right hand, and the experimenter entered the response. Participants were not given any specific instruction about the images. Stimulation sequences were initiated by the experimenter when the participant was ready,

and the EEG recording appeared stable and free of gross artifacts.

2.5. EEG acquisition and preprocessing

The EEG data were collected using 32 Ag/AgCl electrodes positioned according to the 10–20 system (Acharya et al., 2016), with AFz as the ground and the left earlobe as the reference. The EEG signal was recorded at a sampling rate of 1000 Hz using a BrainAmp DC amplifier (Brain Products GmbH, Gilching, Germany). A hardware bandpass filter with a passband of .016–250 Hz was applied during recording and electrode impedances were kept below 10 kΩ.

2.6. Data analysis and statistics

2.6.1. EEG preprocessing

EEG data were preprocessed in MATLAB (version R2023a) using the EEGLAB toolbox (Delorme und Makeig 2004) and custom scripts. Initially, data were resampled to 500 Hz and bandpass filtered with a sinc FIR filter between .1 and 45 Hz (6 dB cut off at .05 and 45.05 Hz, .1 Hz transition bandwidth, using EEGLAB's *pop_eegfiltnew* function). To identify bad channels, the data were segmented into non-overlapping 2-s epochs. Electrodes were removed if more than 15% of such epochs had a standard deviation below 1 μV (indicating a 'dead' segment), or a standard deviation above 250 μV or a range exceeding 500 μV (indicating high-noise segments).

Recordings were subsequently average referenced. Independent Component Analysis was employed to remove common biological artefacts (using EEGLAB's *pop_runica* function with the *Infomax* algorithm). Artifact components were identified using the ICLabel classifier (Pion-Tonachini et al., 2019). Components were considered as isolating an artefact source and removed if the classifier indicated a probability exceeding .9 for the categories of muscle, eye, or heart artifacts. On average 2.4 components were removed per subject (SD: 1.5, range: 0–6). After the removal of artifactual components, previously rejected channels were interpolated using spherical interpolation (EEGLAB's *pop_interp* function). Two CC participants had 2 channels interpolated each, one MCC participant had 1 channel interpolated.

2.6.2. Regions of interest (ROI)

We limited our analysis to the posterior occipital and parieto-temporal channels, which typically yield the strongest responses in this paradigm (e.g., Jacques et al., 2016; Rossion et al., 2015). We selected three regions of interest. First, for analyzing the response to general visual stimulation at the Base rate, we used an *Occipital ROI* comprising channels O1 and O2, as these channels along with Oz, feature the highest response to periodic presentation of visual stimuli (Retter & Rossion, 2016; Rossion et al., 2015). Second, for the analysis of stimulation at the Face rate, we used two lateral posterior ROIs. The *Left ROI* included channels P3, P7, O1, while the *Right ROI* consisted of P4, P8, O2. Lastly, for harmonic selection (see next section) we used a posterior *bilateral ROI* which comprised all channels of the Occipital, Left and Right ROIs (P3, P7, O1, P4, P8, O2).

2.6.3. Spectral analysis and harmonic selection

Data for each trial were segmented between 2 and 42 sec after the beginning of the sequence, thus excluding the fade-in and fade-out segments. Recorded sequences within the same condition and participant were averaged in the time domain before calculating the amplitude spectrum for each channel. The amplitude spectra were computed using MATLAB's periodogram function, configured to output power values which were then square rooted to obtain amplitude values. This analysis, performed on 40-s segments at 500 Hz, results in a high frequency resolution of .025 Hz, capturing all harmonics of both the Base (6, 12, 18, … Hz) and Face (1.2, 2.4, 3.6, … Hz) rate.

For harmonic selection, and to evaluate the presence of responses at the individual level, z-scores were calculated for each harmonic of the Base (6, 12, 18, 24, 30, and 36 Hz) and Face rate (1.2, 2.4, 3.6, 4.8, 7.2, 8.4, 9.6, 10.8, 13.2, 14.4, 15.6, 16.8 Hz). Z-scores were derived by subtracting from each frequency bin, the mean amplitude of 20 neighboring frequency bins (excluding the two immediately adjacent bins) and next dividing by the standard deviation of the same 20 bins (e.g., Rossion et al., 2015; Yan et al., 2019). For example, the 6 Hz z-score was obtained using the mean and standard deviation of bins 5.725–5.95 Hz and 6.05–6.275 Hz. Harmonics were selected based on z-scores calculated from the average spectrum across all participants in the posterior lateral ROI. Harmonic frequencies with a z-score above 3.09 ($p = .001$, one-tailed, see e.g., Jacques et al., 2016; Rossion et al., 2015), indicating a strong signal, were selected for further analysis (see Fig. 1b). This procedure identified harmonics at 6, 12, 18, 24, and 30 Hz for the Base rate and harmonics at 1.2, 2.4, 3.6, 4.8, 7.2, 8.4, 9.6 and 10.8 Hz for the Face rate.

Additionally, z-scores were used to determine individual participants' response to Base and Face stimulation. Participants exhibiting a strong signal at any of the selected harmonic frequencies in any channel, that is those with a z-score value above 4.5 ($p \sim .000002$), were considered to have shown a response to the stimulation. This conservative high threshold for detecting a signal was employed using a Bonferroni correction taking in account the multiple comparisons resulting from the number of channels (32), participants (18 CC + 16 DC +13 MCC = 47) and harmonics tested (8 Face and 5 Base).

2.6.4. Sum of baseline-corrected responses

Differences in the response to different conditions and at different region of interests were evaluated using the sum of baseline-corrected harmonics (Retter et al., 2021; Retter & Rossion, 2016). The mean amplitude of the 20 surrounding frequency bins (excluding the two immediately adjacent bins, as in the z-score calculation) was subtracted from each harmonic frequency. Baseline corrected values were summed across the selected harmonics for the Base and Face rates (Retter et al., 2021), as described in the previous section. In the present manuscript, we refer to these sums of baseline-corrected harmonics for the Base and Face rates as the Base and Face-selective responses, respectively.

2.6.5. Estimated change of face-selective responses due to blurring

The Face-selective response of CC participants was compared to an estimate of how much MCC participants' Face-selective response would decrease if they had the visual acuity of CC participants. This estimate was based on data from Quek et al. (2018) who used a similar FPVS paradigm as in the present study to assess how low-pass spatial filtering of the images affects Face-selective responses in individuals with normal visual development.

CC participants had a mean logMAR acuity of .89 (see Table 1), which corresponds to an image blurring after applying a low-pass filtering with an upper cutoff of approximately 3.8 cycles per visual degree (cpd) [cutoff = 30*10^(-logMAR)]. From Queck et al.'s Fig. 4c we calculated the approximate ratio between Face-selective responses to images filtered at 2.56 cpd, corresponding to the blurring experienced with a visual acuity of logMAR ~1.07 (worse than CC participants' average acuity), and responses to unfiltered images. This resulted in ratios of .428 for a left ROI and .548 for a right ROI, indicating that in Quek et al. (2018) low-pass filtered images at a 2.56 cpd upper cutoff resulted in responses that were 42.8% and 54.8% of the response to the full spectrum image, respectively. By multiplying MCC participants' *left* and *right ROI* Face-selective response by these ratios, we estimated how much their response would theoretically decrease if they experienced visual blurring matching a visual acuity that was (even) worse than the acuity of the present CC participants. These blur-adjusted estimates were statistically compared to the actual Face-selective responses observed in CC participants.

2.6.6. Normalization of Face-selective responses

We further normalized the Face-selective response in two ways. The first normalization was done to compare scalp topography patterns between groups independent of response magnitude (Dzhelyova et al., 2016; Jacques et al., 2016; Yan et al., 2019). For each participant, we first represented the Face-selective response values across all 32 channels as a 32 dimensions vector. We next calculated the L2-norm (Euclidean length) of this vector. Each channel's Face-selective response value was divided by the L2-norm (McCarthy & Wood, 1985). This normalization ensures that the resulting vector has a length of 1, while preserving the relative amplitude contribution of each channel. Consequently, this normalization makes possible to compare topographies across groups, independent of overall amplitude differences which could mimic differences in scalp distribution.

The second normalization was to determine whether group differences in Face-selective response values reflected genuine face processing differences rather than general visual processing differences. This second normalization consisted in a similar rescaling of the Face-selective response values as for the spatial normalization but considering the values of the Base response rather than the overall amplitude of the Face-selective response. Thus, the Base response values across all 32 channels were used as a multidimensional vector and the same procedure as for spatial normalization was applied: The L2-norm of this Base response vector was calculated, and each channel's Face-selective response was divided by the Base response L2-norm. This normalization controls for amplitude differences that might arise from general visual mechanisms shared between face and non-face natural stimulus processing.

2.6.7. Statistical analysis

Linear mixed-effects models (using MATLAB's *fitlme* function) were used to assess the differences in Face-selective and Base responses, with participants as random effect, and covariates for each participant's age, logMar visual acuity and gender.

To compare Base response values between groups, we calculated a model with the fixed-effect factors *Group* (3 levels: CC, DC and MCC) and *Condition* (2 levels: natural and phase-scrambled images), along with their interactions and the three covariates [in Wilkinson's notation: *Base response ~ Group x Condition + Age + Gender + logMar_acuity + (1|subjects)*].

For Face-selective response values, we additionally included each participant's Base response value as a covariate to test whether differences in Face-selective values were independent of general visual mechanisms shared between face and non-face natural stimulus processing. We analyzed a model that included the fixed-effect factors *Group* (3 levels: CC, DC and MCC), *Condition* (2 levels: faces and phase-scrambled images) and ROI (2 levels: Left and Right), along with their interactions and the four covariates [in Wilkinson's notation: *Face-selective response ~ Group x ROI x Condition + Age + Gender + logMar_acuity + Base response +(1|subjects)*].

For the analysis of the Face-selective values normalized by Base response values, we used the same model but without the Base Response covariate, since this was accounted for by the normalization [in Wilkinson's notation: *Face-selective response ~ Group x ROI x condition + Age + Gender + logMar_acuity + (1|subjects)*]. These two analyses, the one with Face-selective values with the Base response covariate and the one with Face-selective values normalized by Base response values, are in fact somewhat redundant but not equivalent. In the first case, differences in Face-selective values at the left and right ROI are controlled by the Base response values at the occipital ROI. In the second case, before calculating the Face-selective values at left and right ROI, the overall Face-selective response across all electrodes was normalized by the overall Base response.

For comparing the scalp topographies between groups, pairwise group comparisons were conducted at each electrode using unpaired two-samples *t*-tests. To account for multiple comparisons across electrodes, the false discovery rate (FDR) correction was applied (Benjamini & Hochberg, 1995; Benjamini & Yekutieli, 2001), with the "bound" *q* set to .05.

2.6.8. Time series analysis

The face categorization response was also evaluated in the time-domain. The preprocessed data were further down sampled to 250 Hz and notch-filtered to remove the responses to non-face stimuli (e.g., Retter & Rossion, 2016; Rossion et al., 2015; Yan et al., 2019). The first six harmonics of the Base rate (6, 12, 18, 24, and 30 Hz) were sequentially bandstop filtered using sinc FIR filters with a .05 Hz transition bandwidth. The data were then segmented from −167 and 836 msec relative to

the presentation of each face stimulus (including one face stimulus preceded by one non-face stimulus and followed by five non-face stimuli). Finally, segments were averaged per condition (face and phase-scrambled) and baseline-corrected to the period from −167 to 0 msec before the appearance of the face stimulus.

At the group level, deviation from 0 μV in the condition averages was evaluated at each time sample and channel using a two-tailed *t*-test. To control for the family-wise error rate from these multiple tests, a cluster-based permutation test was used (Maris & Oostenveld, 2007). Significant t-values (alpha = .05) were clustered based on scalp and time proximity, and the sum of the corresponding t-values was used as the cluster statistic. These cluster values were compared to the highest cluster values obtained in 2000 sample permutations. The permutations were generated by randomly flipping the sign of each participant's averaged data across all channels and time points (Good, 2000; Ossandón et al., 2020). A cluster was considered significant if its statistic value was below the 2.5th percentile or above the 97.5th percentile of the permutation distribution values.

To evaluate differences in time-series deflection latencies, a 50% fractional area latency ($Latency_{50\%}$) measure was employed, utilizing a jackknife method for the estimation of standard errors (se_j) and Welch's *t*-test static for the inter-group comparisons (Kiesel et al., 2008; Miller et al., 2009; Ulrich & Miller, 2001).

2.6.9. *Open data and code availability*

The code for the statistical analyses, figures, and the anonymized, pre-processed data are available at the Research Data Repository of the University of Hamburg (http://doi.org/10.25592/uhhfdm.16128). Original EEG datasets are available upon reasonable request from the corresponding author.

3. Results

A subset of the CC participants (11 out of 18) participated in a brief, custom made face categorization test. All of them performed with 100% accuracy, confirming previous reports that face categorization remains intact after sight restoration following congenital blindness.

3.1. *Neural responses to natural stimuli at 6 Hz*

Participants observed fast periodic visual stimulation at 6 Hz, consisting of close-up photographs of various natural stimuli or their corresponding phase-scrambled images. As illustrated in Fig. 2, which shows the 6 Hz response of individual participants at O2, periodically repetitive stimulation consistently produced strong activity across all individuals of all groups at all 6 Hz harmonics, for both the natural and phase-scrambled images.

As expected, these responses were significant at most electrodes but more pronounced at posterior occipital channels (see Fig. 3a). At the individual level, all participants exhibited a strong, significant response to the stimulation in at least one channel or at least one harmonic frequency (see Fig. 3b), reaffirming the efficacy of FPVS paradigms to elicit significant response in individual participants, even with only three sequences per condition and subject. As expected, Base responses are present for both natural and phase-scrambled images. Thus, congenital cataract-reversal individual, as both control groups, exhibited clear neural responses to fast periodic visual stimulation.

To evaluate differences in the amplitude of response to the 6 Hz visual stimulation, we analyzed the Base response values (participants' sum of baseline corrected harmonics of the Base rate, see methods) using a linear mixed-effect model (see Fig. 3c). This model included fixed effects for *Group* (CC, DC,

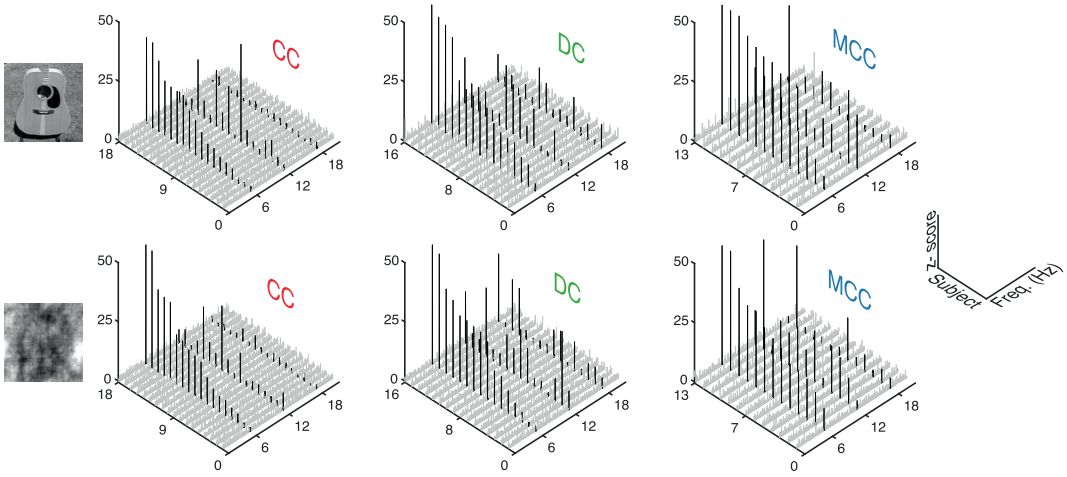

Fig. 2 – Individuals' EEG response to natural stimuli presented at 6 Hz (Base response). Individual spectral responses of each participant at electrode O2 for all groups (CC – congenital cataract-reversal; DC – developmental cataract-reversal; MCC – matched control) and conditions (*top*: natural; *bottom*: phase-scrambled images). Each line represents one participant's z-score of his/her amplitude spectral response at electrode O2. Frequencies corresponding to the harmonics of stimulation (here shown are the three first harmonics: 6, 12 and 18 Hz) are highlighted in black. Participants were sorted by their z-score value at 6 Hz to facilitate visualization.

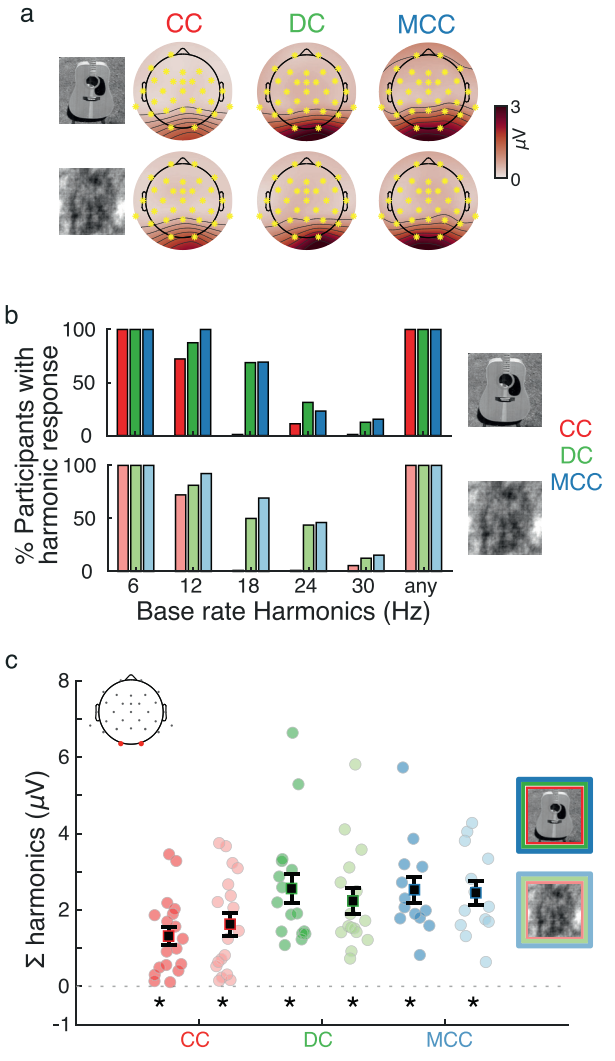

Fig. 3 – EEG response to natural stimuli presented at 6 Hz (Base response). (a) Topographical plots for the group averages of the Base response. Yellow asterisks indicate electrodes in which the values were significantly different from zero (FRD corrected, $q = .05/3$). (b) Percentage of participants per group and condition exhibiting a significant Base response harmonic (z score >4.5) in at least one channel at each harmonic frequency. The rightest bars show the percentages of participants exhibiting a significant Base response in at least one channel and one of the harmonics. (c) Base response for each participant in each of the groups and conditions at the occipital ROI, along with respective averages and s.e.m. Asterisks below the dotted line indicate that the respective values per condition and group were significantly different from zero (all *p*-values <.0001, $\alpha = .05/6$).

and MCC), *Condition* (natural and phase-scrambled image), their interactions, and covariates for *Age*, *Gender*, and *logMar acuity*. The results revealed no significant effect for any of the fixed effects [*Group* $F_{(2,83)} = 1.9$, $p = .15$; *Condition* $F_{(1,83)} = .15$, $p = .69$; *Group x Condition* $F_{(2,83)} = 2.44$, $p = .09$]. Only a significant effect for the *Age* covariate was found [$F_{(1,83)} = 599$, $p = .016$, see Suppl. Fig. 2]. Numerically, however, the mean Base response of the CC group was reduced by 40,8% compared to the MCC group and by 38,6% compared to the DC group.

There was no correlation between the Base response at the occipital ROI and CC participants' visual acuity or age at surgery (see Suppl. Fig. 3, *left* and *middle* panels). The Base response was negatively correlated with the duration since surgery (see Suppl. Fig. 3 right panels), both for natural ($r = -.53$, $p = .023$) and phase-scrambled images ($r = -.53$, $p = .024$). This was not the case for the DC group (all $p > .05$).

3.2. *Face-selective responses*

Faces were presented every fifth stimulus, that is, at a rate of 1.2 Hz. As shown in Fig. 4, participants of all groups exhibited a response at this rate and its harmonics when presented with face stimuli but not for phase-scrambled images.

Face-selective responses were strongest at lateral posterior channels (see Fig. 5a). For individual participants, we observed that 77.7% (14/18) of the CC participants exhibited at least one significant Face rate harmonic to face stimulation in at least at one channel (see Fig. 5b top panel), while 100% of DC and MCC participants did. In contrast, when presented with phase-scrambled stimuli, participant from all tree groups barely showed a significant response at any of the harmonics (see Fig. 5b, lower panel).

To evaluate differences in the amplitude of the response to this 1.2 Hz visual stimulation, we analyzed the Face-selective response values (participants' sum of baseline corrected harmonics of the Face rate, see methods) using a linear mixed-effect model (see Fig. 5c). This model included fixed effects for *Group* (CC, DC, and MCC), *Condition* (faces and phase-scrambled images), *ROI* (left and right parieto-occipital), their interactions, and covariates for participants' *Base response*, *Age*, *Gender*, and *logMar acuity*. The results revealed significant main effects for *Group* [$F_{(2,168)} = 3.73$, $p = .026$], *Condition* [faces > phase-scrambled, $F_{(1,168)} = 260.3$, $p < .0001$] and *ROI* [right > left, $F_{(1,168)} = 4.7$, $p < .032$]. Additionally, there were significant interactions for *Group x Condition* [$F_{(2,168)} = 38.5$, $p < .0001$] and *ROI x Condition* [$F_{(1,168)} = 4.6$, $p = .03$]. Only the covariate for age was significant [responses decreased with age, $F_{(1,168)} = 9.3$, $p = .003$, see Suppl. Fig. 4]. Groups significantly differed only for natural faces and not for the phase-scrambled versions of these images, with the CC group showing much smaller values that the MCC ($p < .0001$) and the DC group ($p < .0001$), representing a 75.4 % and 79% amplitude reduction, respectively. In contrast, MCC and DC groups did not differ ($p = .3$) (see Fig. 5e). The right lateralization (difference between right and left ROI) was significantly larger for faces than phase-scrambled images ($p = .03$) (see Fig. 5f).

Apart from establishing that CC participants' Face-selective response was lower than in the control groups, even when taking in account their reduced visual acuity and reduced Base response, we evaluated whether CC participants' reduced Face-selective response differed from what would be expected due to possible blur caused by their visual acuity deficits. We compared Face-selective responses of the CC group to a blur-adjusted estimate of MCC participants'

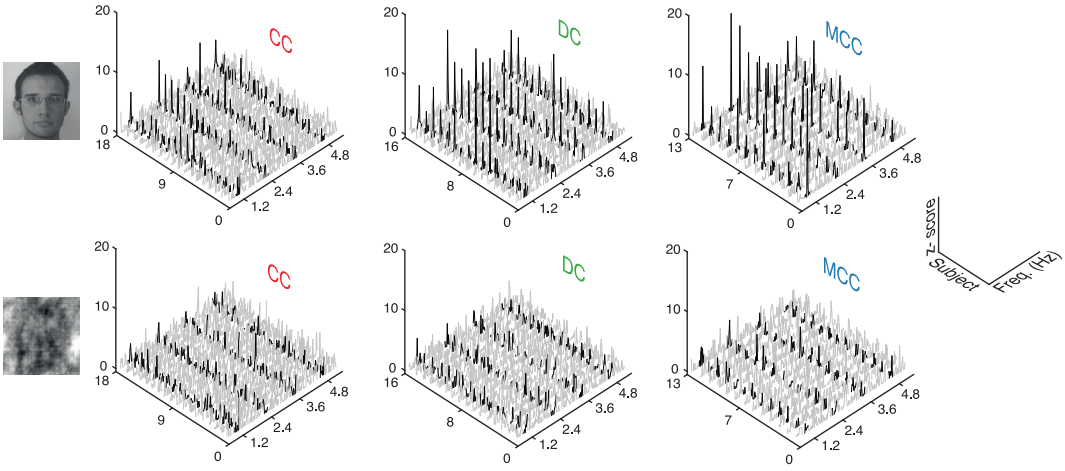

Fig. 4 – Individuals' EEG response to face stimuli presented at 1.2 Hz (Face-selective responses). Individual spectral responses of each participant at electrode P8 for the different groups and conditions (*top*: face; *bottom*: phase-scrambled images). Participants were sorted by their z-score value at 2.4 Hz (the harmonic with highest values) to facilitate visualization.

Face-selective responses. Blur level was selected such that it matched a visual acuity lower than CC participants' visual acuity (horizontal orange lines in Fig. 5c, see methods section 2.6.5 for details). CC participants' Face-selective responses were still significantly lower than the blur adjusted Face-selective response of MCC participants for both ROIs [left ROI: CC: .36 *vs* MCC blur adjusted: .67, $t_{(17)}$: −4.03 $p = .001$; right ROI: CC: .52 *vs* MCC blur-adjusted: 1.1, $t_{(17)}$: −4.08 $p = .001$]. Thus, the reduced Face-selective response of CC participants cannot be explained by their reduced visual acuity.

To investigate whether there were differences in scalp distribution in the response to face stimuli, which would suggest that EEG responses in CC individuals originated from different neural sources, we performed a spatial normalization of the Face-selective response values (see methods section *Normalization of Face responses*). Fig. 5d displays the resulting topographies and their group differences. No significant differences across channels were found between any of the groups ($p > .05$, FDR corrected), indicating that the scalp topographies of the face-categorization response did not differ across groups and thus might origin from indistinguishable sources.

The reduction for Face-selective responses in the CC group was approximately twice as large as the reduction for Base responses when compared to the MCC group (75.4% *vs* 40.8% reduction, respectively) suggesting a specific decline for face-selective processing, independent of visual processes shared with other types of object processing, such contour integration or figure/background segmentation. In addition to the analysis above showing that the Base response covariate did not explain differences in Face-selective responses in the CC Group we next evaluated whether the lower Base response accounted for this group difference. To this end the Face-selective responses were normalized by the Base responses across the scalp (see methods section 2.6.6 *Normalization of Face-selective responses*). We submitted the resulting normalized values to the same linear-mixed model described previously for the analysis of the non-normalized values, this time without the Base response covariate. The results revealed a significant main effect of *Condition* [faces > phase-scrambled images, $F_{(1,169)} = 165.8$, $p < .0001$] and a significant interaction of *Group* x *Condition* [$F_{(2,169)} = 12.4$, $p < .0001$]; the main effect of Group was not significant [$F_{(2,\ 169)} = 2.66$, $p = .07$] nor was *ROI* [$F_{(1,\ 169)} = 2.9$, $p = .09$]. Additionally, the covariate of age was significant [response decreasing with age, $F_{(1,168)} = 6.4$, $p = .012$]. The *Group* × *Condition* interaction was driven by a significant group difference for face images but not for phase-scrambled images; the CC group had smaller values for the Face-selective response to intact face stimuli than the MCC ($p = .009$) and the DC group ($p = .0009$), while the MCC and DC groups did not differ ($p = .24$) (see Fig. 5g). Thus, these results confirm the results of the analysis of non-normalized Face-selective values. Hence, differences between groups observed for the Face-selective response cannot be explained neither by differences in the processing of low-level differences between faces and other natural images, nor by high-level visual mechanism that are common for the processing of faces and other natural stimuli.

There was no correlation between the Face-selective response at the right ROI and CC participants' visual acuity, age at surgery, or duration since surgery (see Suppl. Fig. 5).

3.3. *Time domain analysis*

We examined the temporal dynamics of face categorization by analyzing time-series averages aligned with each face presentation, while controlling for signals related to the Base rate (see methods section *Time series analysis*). A cluster-based permutation test identified significant positive and negative deflections in all three groups, illustrated in Fig. 6a. Specifically, the CC and MCC group each exhibited one positive and one negative cluster, whereas the DC group displayed an additional positive cluster starting earlier. The negative and positive clusters found in all three groups are in accord with

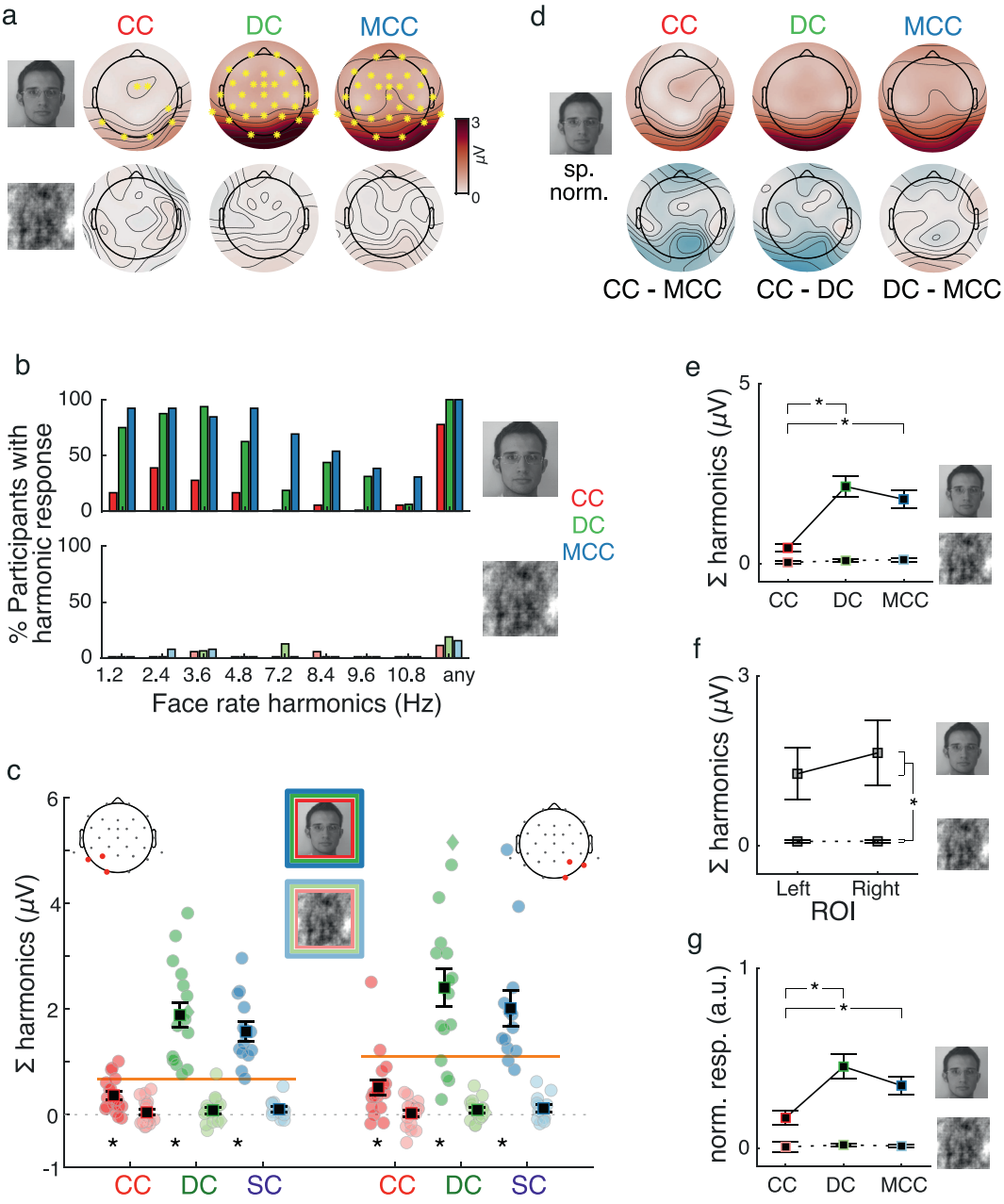

Fig. 5 – EEG response to face stimuli presented at 1.2 Hz (Face-selective responses). (a) Topographical plots illustrating the group average face response for both face (*top*) and phase-scrambled stimuli (*bottom*). Yellow asterisks indicate electrodes at which the values were significantly different from 0 (FRD corrected, $q = .05/3$). (b) Percentage of participants per group and condition exhibiting a significant Face rate harmonic (z score >4.5) in at least one channel at each harmonic frequency. The rightest bar shows the percentage of participants exhibiting a significant Face-selective response in at least one channel and one of the harmonics. (c) Face response for each participant in each group, condition, and occipital-parietal ROI. Dark colors represent face stimuli, while light-colors indicate phase-scrambled stimuli. The horizontal orange line indicates the blur-adjusted estimate of MCC response (per ROI). Asterisks indicate that the respective values per condition and group were significantly different from zero (all *p*-values <.003, $\alpha = .05/12$). The green diamond indicates a DC participant with nystagmus. (d) Topographical plots (in normalized amplitude) showing the group averages of spatially normalized values (*top*) and the differences between groups (*bottom*). No difference between groups was observed across the scalp for the spatially normalized values. (e) Group × Condition interaction: Comparison between groups for each condition. (f) ROI × Condition interaction: Comparison between conditions for each hemisphere. (g) Group × Condition interaction for Face-selective values normalized by Base response values.

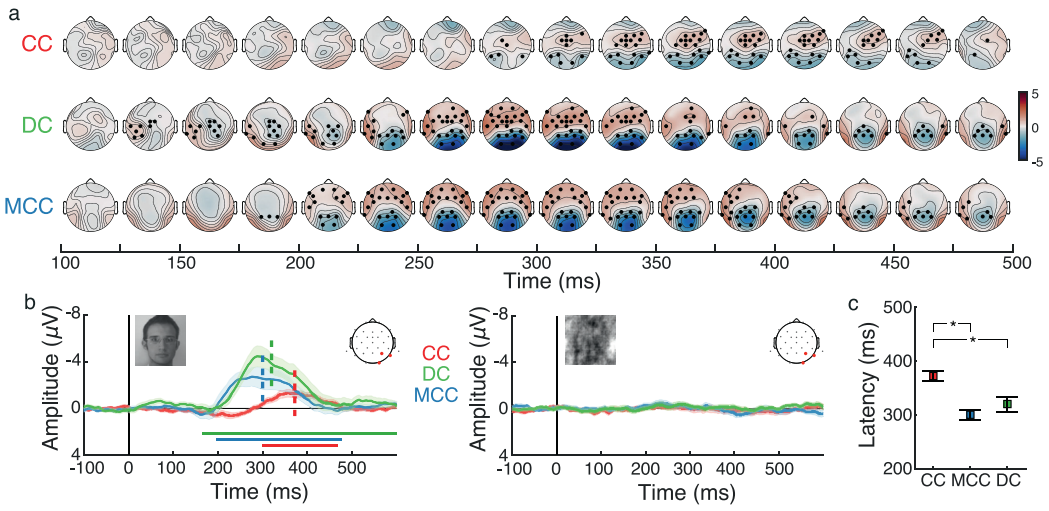

Fig. 6 – Time domain analysis. (a) Topographic plot succession of time series responses locked to face presentation (i.e., deviations from the common response of faces and objects). Black dots indicate electrodes belonging to a significant cluster at a given time point (in 25 msec windows). (b) Time series averages at the right ROI for faces (left) and phase-scrambled (right) stimuli. Vertical dotted lines (left and middle panel) indicate the latency of the negative deflection as defined by the 50% fractional area latency measure. Horizontal colored lines at the bottom indicate time points in which the deflection at this ROI, was significantly different from 0 according to the cluster-based permutation test. (c) Estimates of $Latency_{50\%}$ per group. Error bars are jackknife-based standard errors. Asterisks indicate significant difference between groups ($\alpha = .05/3$).

the previously observed negative defection to faces ("N1-Faces") over posterior occipito-temporal regions, along with a corresponding anterior positive counterpart (Retter et al., 2020; Retter & Rossion, 2016).

Furthermore, as seen in Fig. 6b for the right ROI, these deflections were present solely in response to face stimuli (Fig. 6b, left panel) but not for phase-scrambled stimuli (Fig. 6b, right panel), confirming that the negative deflection to faces indicates genuine face-selective neural processes.

The onset latency of the time domain deflection was longer in the CC group than in both the MCC and DC groups. The negative deflection observed in all groups emerged significantly later in the CC compared to the MCC and DC group [see Fig. 6c ($Latency_{50\%}$ CC: 372 msec, se_j: 9.5; MCC: 300 msec, se_j: 9.4; DC: 320 msec, se_j: 14; CC *vs* MCC $t_{(28.2)} = 5.4$, $p < .0001$; CC *vs* DC $t_{(27.0)} = 3.2$, $p = .002$; MCC *vs* DC $t_{(25.2)} = -1.1$, $p = .8$]. In conclusion, the different temporal dynamics of the face categorization response in CC individuals suggested a delayed categorization response in the CC group than in both the DC and MCC group. As a note, we did not analyze the amplitude of the time domain response since the obviously lower amplitude in the CC group corresponds in the context of fast periodic stimulation by and large to their lower amplitude (sum of harmonics) of the Face rate response in the frequency domain.

4. Discussion

Individuals who regained sight after a transient period of congenital blindness have consistently exhibited impairments in face individuation while being able to categorize sensory stimuli as faces. Here, we used frequency-tagging to rigorously assess fast and automatic face categorization in sight-recovery individuals who had experienced long-term congenital visual deprivation. These participants apparently displayed intact behavioral face-categorization, as evidenced by a behavioral screening. However, the amplitude of the Face-selective response was markedly reduced in congenital cataract reversal individuals compared to normally sighted controls (reduction by ~75 %) as well as compared to individuals with reversed developmental cataracts (reduction by 79%). Moreover, the Face-selective response of congenital cataract reversal individuals was lower than what would have been expected by their reduced visual acuity. The difference between congenital cataract reversal and the two other groups remained significant even after controlling for their overall reduced neural response to visual flickering stimuli. Moreover, potential scalp topography differences did not account for the overall lower Face-selective response of individuals with reversed congenital cataracts. Time-domain EEG analysis further revealed a longer onset latency of Face-selective activity in congenital cataract reversal individuals compared to both control groups. Thus, the present study uncovers yet overseen weaknesses in (neural) face categorization in individuals with reversed congenital cataracts.

As in most previous studies employing frequency tagging EEG methods to study face categorization (e.g., de Heering & Rossion, 2015; Jacques et al., 2016; Liu-Shuang et al., 2016; Rossion et al., 2015), we presented the face and non-face stimuli at a relatively high temporal rate (6 Hz). The Face-selective response indicates genuine neural face categorization, rather than other types of visual processing, since a Face-selective response can only emerge if participants have reliably detected the face images in the stream on non-face stimuli. Since faces were embedded in natural backgrounds and varied across several dimensions, such as in viewpoint and lighting, a Face-selective response was unlikely due to low-level features. This conclusion is supported by the lack of

such a response for phase-scrambled images, as replicated in the present study too. In fact, the Face-selective response has been shown to be present with even more heterogenous face stimuli (e.g., Quek et al., 2018). As successful face categorization required the ability to quickly process and segment images, individuals must have been able to reliably categorize faces at "a single glance" to generate a significant response (Liu-Shuang et al., 2016; Retter & Rossion, 2016). Here we provide strong evidence that most congenital cataract reversal individuals successfully mastered this challenge. This result is compatible with preliminary studies indicating that sight-recovery individuals with a history of long-lasting congenital blindness exhibited successful behavioral visual categorization abilities (Gandhi et al., 2017; Ossandón et al., 2022; Ostrovsky et al., 2009; Röder et al., 2013). As discussed earlier, congenital cataract reversal individuals' Face-selective response was indistinguishable in scalp topography from that of normally sighted controls, that is, a right lateralized posterior distribution was observed. Earlier studies have demonstrated that this topography is not found for other categories (Jacques et al., 2016), and that this activity emerges from face selective parts of the ventral occipito-temporal cortex (Hauk et al., 2021; Jonas et al., 2016). Moreover, the Face-selective response is highly correlated with behavioral detection performance for faces (Retter et al., 2020). These lines of evidence converge to the conclusion, that the Face-selective response, as measured in the present study, reflects genuine face categorization processes rather than the detection of mere low-level regularities distinguishing faces from other object categories. Finally, it could be argued that low-level regularities of the faces might have induced some learning effects independent of face categorization. We consider this explanation as unlikely, since only three sequences of natural stimuli per experiment were presented. Such learning effects would require detecting low-level features shared by face images but not for other object categories. As argued before, the latter account is highly unlikely, and thus, all learning, if learning played a role at all, would have emerged from face categorization.

With neural measures we did find differences in face categorization between congenital cataract reversal individuals compared to both normally sighted controls and developmental cataract reversal individuals. The reduced amplitude of the frequency-tagged response to faces and the longer latency of the time-domain face response in individuals with reversed congenital cataracts suggest a smaller or less well-coordinated neural circuit dedicated to face processing and reduced neural processing efficiency, respectively. Longer latencies of the face response in the time domain are reminiscent of findings in infants who exhibit a face-selective ERPs with much longer delays than adults (e.g., Conte et al., 2020).

In a previous face categorization frequency-tagging experiment, it was demonstrated that the amplitude of the face-categorization response decreased with higher stimulation rates (Retter et al., 2020). This decrease correlated with the participants' ability to explicitly detect faces and was considered to be a consequence of to be able or not at all be able to categorize singular faces under high presentation rates. The reduced amplitude observed for the Face-selective response in congenital cataract reversal individuals may thus be due to a lower likelihood to successfully classify faces. Reasons could be the less efficient processing in these neural circuits (see longer latencies of the Face effect in the time domain analysis) or less face selective neural circuits (as discussed in the next paragraph).

We assume that neural circuits typically selectively activated by faces are more activated by non-face stimuli in congenital cataract reversal individuals. This account aligns well with the reduced selectivity of typical face-selective regions in VOTC (specifically the fusiform gyrus) which has recently been observed with fMRI in an independent group of congenital cataract reversal individuals (Rączy et al., 2024). In this fMRI study, the authors speculated, in agreement with previous electrophysiological studies (Röder et al., 2013), that the reduced face selectivity of typical face processing regions were the consequence of a lack of experience-based tuning, which in typical development causes neural circuits to specialize and consecutively respond less to the non-preferred category (Cantlon et al., 2011; Livingstone et al., 2017). Here, we further show that reduced selectivity is accompanied by less efficient processing, as evidenced by the longer latency of the Face-selective response in the time domain (see the above discussion of the longer latency for the face response in the time domain).

We have recently proposed that the lack of typical face-selective areas in congenital cataract reversal individuals might be related to their impoverished representation of the central visual field and degraded feature pooling across visual areas (Rączy et al., 2024). This view was based on a recent high-field fMRI study demonstrating that congenital cataract reversal individuals had larger population receptive fields and a smaller cortical magnification factor in primary visual cortex for the foveal part of the visual field (Heitmann et al., 2023). A preserved representation of the center of the visual field is consider essential for face processing, as face-selective areas in humans and monkeys typically show a foveal bias (Arcaro & Livingstone, 2017; Finzi et al., 2021; Gomez et al., 2018; Hasson et al., 2002; Lafer-Sousa & Conway, 2013). This foveal bias in higher order visual cortex has been shown to be present but only coarsely tuned to face-like stimuli soon after birth (Arcaro & Livingstone, 2017), and was proposed to provide the scaffold for the final fine tuning for faces (Livingstone et al., 2017). We hypothesize that the degraded neural representation of the fovea in primary visual cortex of congenital cataract reversal individuals impedes the necessary pooling of features in downstream regions. In turn, proper tuning of these downstream areas may be essential for the processing of configural face information, where the spatial relationship between facial features – rather than the features themselves – is crucial (Poltoratski et al., 2021). In fact, individuals with reversed congenital cataracts seem to suffer from a particular impairment in "holistic" face processing (Le Grand et al., 2004) which in turn is crucial for face individuation.

Ideally, we would have included a condition where instead of faces other object categories had been regularly repeated every at 1.2 Hz. This would have allowed us to decide whether categorization of other visual categories is associated with the same neural impairments as categorization of faces. Based on the fMRI study of Raczy et al. (2024) we predict a null result,

that is, no difference between congenital cataract reversal individuals and normally sighted controls for other categories. Using different operationalization methods of category selectivity, Raczy et al. (2024) demonstrated impaired selectivity in VOTC for face processing but spared category selectivity for other categories such like places.

It could be argued that congenital cataract reversal individuals exhibit a Face-selective response with lower amplitude because of persisting impaired visual acuity or the presence of nystagmus. Although visual evoked potentials (VEP) and steady state visual evoked potential (SSVEP) amplitudes decrease with lower visual acuity (Bach et al., 2008; Jeon et al., 2012), we provide evidence that these factors do not account for the reduced Face-sensitive response of congenital cataract reversal individuals in the present study: First, the Face-selective response was significantly more impaired than the Base response; even when visual acuity was included as a covariate group differences remained significant. Second, the diminished Face-selective response of individuals with reversed congenital cataracts was more severe than what would have been expected from optically blurring images to a degree corresponding to this group's visual acuity. Third, we additionally tested individuals who had experienced partially severe visual impairment later in childhood due to developmental cataracts before receiving the same treatment as congenital cataract reversal individuals. Despite persisting visual acuity loss post-surgery too, these developmental cataract reversal individuals exhibited neither a reduction of their Base rate nor of their Face-rate response. Finally, we were unable to detect any correlation between visual acuity and the amplitude of the Face-selective response in individuals with reversed congenital cataracts.

Earlier studies reported reduced visual evoked potentials in individuals suffering from nystagmus (Kelly et al., 2021; Quanz et al., 2024; Saunders et al., 1997). The amplitude reduction was found to depend on the timing of stimulus presentation relative to the foveation periods within the nystagmus (Dunn et al., 2023; Kelly et al., 2017, 2021). Recently, Quanz et al. (2024) used SSVEPs to assess visual acuity in patients suffering from nystagmus. They found that reduction of the SSVEP amplitudes were linearly related to a loss of visual acuity. In contrast, we did not observe correlation between visual acuity and the Face-selective response in congenital cataract reversal individuals. Moreover, as discussed earlier, the expected image blur in this group did not account for the degree of amplitude loss for the Face-selective response. Nevertheless, in this context, including a third control group of individuals with nystagmus who have not experienced congenital visual deprivation would have been beneficial.

In conclusion, the present results demonstrated that individuals with reversed congenital cataracts possess neural circuits for rapid and automatic face categorization. However, these neural circuits appear to function less efficiently in this group, presumably due to their lower face-selectivity. Future behavioral studies should employ more challenging face categorization tasks, such as using more schematic images that further reduce the distinctiveness of faces versus other objects or by increasing the stimulus presentation rate. We predict that successful face categorization would break down earlier in congenital cataract reversal individuals than in controls.

CRediT authorship contribution statement

José P. Ossandón: Writing – review & editing, Writing – original draft, Formal analysis. **Bruno Rossion:** Writing – review & editing, Resources, Conceptualization. **Giulia Dormal:** Writing – review & editing, Investigation, Conceptualization. **Ramesh Kekunnaya:** Writing – review & editing, Resources, Project administration, Investigation. **Brigitte Röder:** Writing – review & editing, Writing – original draft, Supervision, Project administration, Funding acquisition, Conceptualization.

Declaration of generative AI and AI-assisted technologies in the writing process

During the preparation of this work the authors used ChatGPT 4o and Claude 3.7 Sonnet in order to improve readability and language. After using this tool/service, the authors reviewed and edited the content as needed and take full responsibility for the content of the published article.

Declaration of competing interest

The authors declare no conflict of interest.

Acknowledgments

This work was supported by the German Research Foundation (DFG) (grants Ro 2625/10-1 and SFB 936 - 178316478 – B2/B11). We acknowledge financial support from the Open Access Publication Fund of Universität Hamburg. The authors are grateful to D. Balasubramanian who made the research at the LV Prasad Eye Institute possible. We thank Idris Shareef, Siddhart S. Rajendran, Kabilan Pitchaimuthu, Prativa Regmin and Suddha Sourav for helping with data acquisition, Bhavana Kolli for clinical data curation, and Diane Rekow and Katarzyna Rączy for comments on initial drafts.

Supplementary data

Supplementary data to this article can be found online at https://doi.org/10.1016/j.cortex.2025.04.007.

Scientific transparency statement

DATA: Some raw and processed data supporting this research are publicly available, while some are subject to restrictions: http://doi.org/10.25592/uhhfdm.16128.
CODE: All analysis code supporting this research is publicly available: http://doi.org/10.25592/uhhfdm.16128.
MATERIALS: All study materials supporting this research are publicly available: https://face-categorization-lab.webnode.com/resources/natural-face-stimuli/.
DESIGN: This article reports, for all studies, how the author(s) determined all sample sizes, all data exclusions, all data

inclusion and exclusion criteria, and whether inclusion and exclusion criteria were established prior to data analysis.
PRE-REGISTRATION: No part of the study procedures was pre-registered in a time-stamped, institutional registry prior to the research being conducted. No part of the analysis plans was pre-registered in a time-stamped, institutional registry prior to the research being conducted.
For full details, see the *Scientific Transparency Report* in the supplementary data to the online version of this article.

REFERENCES

Abadi, R. V., Forster, J. E., & Lloyd, I. C. (2006). Ocular motor outcomes after bilateral and unilateral infantile cataracts. *Vision Research, 46*(6–7), 940–952. https://doi.org/10.1016/j.visres.2005.09.039

Acharya, J. N., Hani, A. J., Cheek, J., Thirumala, P., & Tsuchida, T. N. (2016). American clinical neurophysiology society guideline 2: Guidelines for standard electrode position nomenclature. *The Neurodiagnostic Journal, 56*(4), 245–252. https://doi.org/10.1080/21646821.2016.1245558

Arcaro, M. J., & Livingstone, M. S. (2017). A hierarchical, retinotopic proto-organization of the primate visual system at birth. *eLife, 6*, Article e26196. https://doi.org/10.7554/eLife.26196

Bach, M., Maurer, J. P., & Wolf, M. E. (2008). Visual evoked potential-based acuity assessment in normal vision, artificially degraded vision, and in patients. *British Journal of Ophthalmology, 92*(3), 396–403. https://doi.org/10.1136/bjo.2007.130245

Benjamini, Y., & Hochberg, Y. (1995). Controlling the false discovery rate: A practical and powerful approach to multiple testing. *Journal of the Royal Statistical Society: Series B (Methodological), 57*(1), 289–300.

Benjamini, Y., & Yekutieli, D. (2001). The control of the false discovery rate in multiple testing under dependency. *The Annals of Statistics, 29*(4). https://doi.org/10.1214/aos/1013699998

Bentin, S., Allison, T., Puce, A., Perez, E., & McCarthy, G. (1996). Electrophysiological studies of face perception in humans. *Journal of Cognitive Neuroscience, 8*(6), 551–565. https://doi.org/10.1162/jocn.1996.8.6.551

Cantlon, J. F., Pinel, P., Dehaene, S., & Pelphrey, K. A. (2011). Cortical representations of symbols, objects, and faces are pruned back during early childhood. *Cerebral Cortex, 21*(1), 191–199. https://doi.org/10.1093/cercor/bhq078

Conte, S., Richards, J. E., Guy, M. W., Xie, W., & Roberts, J. E. (2020). Face-sensitive brain responses in the first year of life. *Neuroimage, 211*, Article 116602. https://doi.org/10.1016/j.neuroimage.2020.116602

de Heering, A., & Maurer, D. (2014). Face memory deficits in patients deprived of early visual input by bilateral congenital cataracts: Face memory deficits in cataract-reversal patients. *Developmental Psychobiology, 56*(1), 96–108. https://doi.org/10.1002/dev.21094

de Heering, A., & Rossion, B. (2015). Rapid categorization of natural face images in the infant right hemisphere. *eLife, 4*, Article e06564. https://doi.org/10.7554/eLife.06564

Dunn, M. J., Carter, P., Self, J., Lee, H., & Shawkat, F. (2023). Eyetracking-enhanced VEP for nystagmus. *Scientific Reports, 13*(1), Article 22812. https://doi.org/10.1038/s41598-023-50367-y

Dzhelyova, M., Jacques, C., & Rossion, B. (2016). At a single glance: Fast periodic visual stimulation uncovers the spatio-temporal dynamics of brief facial expression changes in the human brain. *Cerebral Cortex, 27*, 4106–41213. https://doi.org/10.1093/cercor/bhw223

Finzi, D., Gomez, J., Nordt, M., Rezai, A. A., Poltoratski, S., & Grill-Spector, K. (2021). Differential spatial computations in ventral and lateral face-selective regions are scaffolded by structural connections. *Nature Communications, 12*(1), 2278. https://doi.org/10.1038/s41467-021-22524-2

Gandhi, T. K., Singh, A. K., Swami, P., Ganesh, S., & Sinha, P. (2017). Emergence of categorical face perception after extended early-onset blindness. *Proceedings of the National Academy of Sciences, 114*(23), 6139–6143. https://doi.org/10.1073/pnas.1616050114

Gao, X., Gentile, F., & Rossion, B. (2018). Fast periodic stimulation (FPS): A highly effective approach in fMRI brain mapping. *Brain Structure & Function, 223*(5), 2433–2454. https://doi.org/10.1007/s00429-018-1630-4

Gelbart, S. S., Hoyt, C. S., Jastrebski, G., & Marg, E. (1982). Long-term visual results in bilateral congenital cataracts. *American Journal of Ophthalmology, 93*(5), 615–621. https://doi.org/10.1016/S0002-9394(14)77377-5

Geldart, S., Mondloch, C. J., Maurer, D., De Schonen, S., & Brent, H. P. (2002). The effect of early visual deprivation on the development of face processing. *Developmental Science, 5*(4), 490–501. https://doi.org/10.1111/1467-7687.00242

Gomez, J., Natu, V., Jeska, B., Barnett, M., & Grill-Spector, K. (2018). Development differentially sculpts receptive fields across early and high-level human visual cortex. *Nature Communications, 9*(1), 788. https://doi.org/10.1038/s41467-018-03166-3

Good, P. I. (2000). *Permutation tests: A practical guide to resampling methods for testing hypotheses* (2nd ed.). Springer-Verlag.

Grady, C. L., Mondloch, C. J., Lewis, T. L., & Maurer, D. (2014). Early visual deprivation from congenital cataracts disrupts activity and functional connectivity in the face network. *Neuropsychologia, 57*, 122–139. https://doi.org/10.1016/j.neuropsychologia.2014.03.005

Hasson, U., Levy, I., Behrmann, M., Hendler, T., & Malach, R. (2002). Eccentricity bias as an organizing principle for human high-order object areas. *Neuron, 34*(3), 479–490. https://doi.org/10.1016/S0896-6273(02)00662-1

Hauk, O., Rice, G. E., Volfart, A., Magnabosco, F., Ralph, M. A. L., & Rossion, B. (2021). Face-selective responses in combined EEG/MEG recordings with fast periodic visual stimulation (FPVS). *Neuroimage, 242*, Article 118460. https://doi.org/10.1016/j.neuroimage.2021.118460

Heitmann, C., Zhan, M., Linke, M., Hölig, C., Kekunnaya, R., Van Hoof, R., Goebel, R., & Röder, B. (2023). Early visual experience refines the retinotopic organization within and across visual cortical regions. *Current Biology, 33*(22), 4950–4959.e4. https://doi.org/10.1016/j.cub.2023.10.010

Jacques, C., Retter, T. L., & Rossion, B. (2016). A single glance at natural face images generate larger and qualitatively different category-selective spatio-temporal signatures than other ecologically-relevant categories in the human brain. *Neuroimage, 137*, 21–33. https://doi.org/10.1016/j.neuroimage.2016.04.045

Jeon, J., Oh, S., & Kyung, S. (2012). Assessment of visual disability using visual evoked potentials. *BMC Ophthalmology, 12*(1), 36. https://doi.org/10.1186/1471-2415-12-36

Jonas, J., Jacques, C., Liu-Shuang, J., Brissart, H., Colnat-Coulbois, S., Maillard, L., & Rossion, B. (2016). A face-selective ventral occipito-temporal map of the human brain with intracerebral potentials. *Proceedings of the National Academy of Sciences, 113*(28), E4088–E4097. https://doi.org/10.1073/pnas.1522033113

Kelly, J. P., Phillips, J. O., & Weiss, A. H. (2017). The relationship of nystagmus waveform on the VEP response in infantile nystagmus syndrome: A small case series. *Documenta Ophthalmologica, 134*(1), 37–44. https://doi.org/10.1007/s10633-016-9568-4

Kelly, J. P., Tarczy-Hornoch, K., Phillips, J. O., & Weiss, A. H. (2021). A reduced visual pathway response in infantile nystagmus syndrome. *Journal of American Association for Pediatric Ophthalmology and Strabismus, 25*(1), 9.e1–9.e6. https://doi.org/10.1016/j.jaapos.2020.09.005

Kiesel, A., Miller, J., Jolicœur, P., & Brisson, B. (2008). Measurement of ERP latency differences: A comparison of single-participant and jackknife-based scoring methods. *Psychophysiology, 45*(2), 250–274. https://doi.org/10.1111/j.1469-8986.2007.00618.x

Lafer-Sousa, R., & Conway, B. R. (2013). Parallel, multi-stage processing of colors, faces and shapes in macaque inferior temporal cortex. *Nature Neuroscience, 16*(12), 1870–1878. https://doi.org/10.1038/nn.3555

Lambert, S. R., Lynn, M. J., Reeves, R., Plager, D. A., Buckley, E. G., & Wilson, M. E. (2006). Is there a latent period for the surgical treatment of children with dense bilateral congenital cataracts? *Journal of American Association for Pediatric Ophthalmology and Strabismus, 10*(1), 30–36. https://doi.org/10.1016/j.jaapos.2005.10.002

Le Grand, R., Mondloch, C. J., Maurer, D., & Brent, H. P. (2001). Early visual experience and face processing. *Nature, 412*(August), 26–27.

Le Grand, R., Mondloch, C. J., Maurer, D., & Brent, H. P. (2004). Impairment in holistic face processing following early visual deprivation. *Psychological Science, 15*(11), 762–768. https://doi.org/10.1111/j.0956-7976.2004.00753.x. PSCI753 [pii].

Liu-Shuang, J., Torfs, K., & Rossion, B. (2016). An objective electrophysiological marker of face individualisation impairment in acquired prosopagnosia with fast periodic visual stimulation. *Neuropsychologia, 83*, 100–113. https://doi.org/10.1016/j.neuropsychologia.2015.08.023

Livingstone, M. S., Vincent, J. L., Arcaro, M. J., Srihasam, K., Schade, P. F., & Savage, T. (2017). Development of the macaque face-patch system. *Nature Communications, 8*(1), Article 14897. https://doi.org/10.1038/ncomms14897

Maris, E., & Oostenveld, R. (2007). Nonparametric statistical testing of EEG- and MEG-data. *Journal of Neuroscience Methods, 164*(1), 177–190. https://doi.org/10.1016/j.jneumeth.2007.03.024

Maurer, D., Lewis, T. L., & Mondloch, C. J. (2005). Missing sights: Consequences for visual cognitive development. *Trends in Cognitive Sciences, 9*(3 SPEC. ISS.), 144–151. https://doi.org/10.1016/j.tics.2005.01.006

McCarthy, G., & Wood, C. C. (1985). Scalp distributions of event-related potentials: An ambiguity associated with analysis of variance models. *Electroencephalography and Clinical Neurophysiology, 62*, 203–208.

Miller, J., Ulrich, R., & Schwarz, W. (2009). Why jackknifing yields good latency estimates. *Psychophysiology, 46*(2), 300–312. https://doi.org/10.1111/j.1469-8986.2008.00761.x

Mondloch, C. J., Le Grand, R., & Maurer, D. (2003). Early visual experience is necessary for the development of some–but not all–aspects of FAce processing. In O. Pascalis, & A. Slater (Eds.), *The development of face processing in infancy and early childhood* (pp. 99–117). Nova Science Publishers.

Mondloch, C. J., Segalowitz, S. J., Lewis, T. L., Dywan, J., Le Grand, R., & Maurer, D. (2013). The effect of early visual deprivation on the development of face detection. *Developmental Science, 16*(5), 728–742. https://doi.org/10.1111/desc.12065

Ossandón, J. P., König, P., & Heed, T. (2020). No evidence for a role of spatially modulated α-Band activity in tactile remapping and short-latency, overt orienting behavior. *The Journal of Neuroscience, 40*(47), 9088–9102. https://doi.org/10.1523/JNEUROSCI.0581-19.2020

Ossandón, J. P., Zerr, P., Shareef, I., Kekunnaya, R., & Röder, B. (2022). Active vision in sight recovery individuals with a history of long-lasting congenital blindness. *Eneuro, 9*(5). https://doi.org/10.1523/ENEURO.0051-22.2022. ENEURO.0051-22.2022.

Ostrovsky, Y., Andalman, A., & Sinha, P. (2006). Vision following extended congenital blindness. *Psychological Science, 17*(12), 1009–1014. https://doi.org/10.1111/j.1467-9280.2006.01827.x

Ostrovsky, Y., Meyers, E., Ganesh, S., Mathur, U., & Sinha, P. (2009). Visual parsing after recovery from blindness. *Psychological Science, 20*(12), 1484–1491. https://doi.org/10.1111/j.1467-9280.2009.02471.x

Pion-Tonachini, L., Kreutz-Delgado, K., & Makeig, S. (2019). ICLabel: An automated electroencephalographic independent component classifier, dataset, and website. *Neuroimage, 198*, 181–197. https://doi.org/10.1016/j.neuroimage.2019.05.026

Poltoratski, S., Kay, K., Finzi, D., & Grill-Spector, K. (2021). Holistic face recognition is an emergent phenomenon of spatial processing in face-selective regions. *Nature Communications, 12*(1), 4745. https://doi.org/10.1038/s41467-021-24806-1

Putzar, L., Hötting, K., & Röder, B. (2010). Early visual deprivation affects the development of face recognition and of audio-visual speech perception. *Restorative Neurology and Neuroscience, 28*(2), 251–257. https://doi.org/10.3233/RNN-2010-0526

Quanz, E. V., Kuske, J., Stolle, F. H., Bach, M., Heinrich, S. P., Hoffmann, M. B., & Al-Nosairy, K. O. (2024). Effect of nystagmus on VEP-based objective visual acuity estimates. *Scientific Reports, 14*(1), Article 16797. https://doi.org/10.1038/s41598-024-66819-y

Quek, G. L., Liu-Shuang, J., Goffaux, V., & Rossion, B. (2018). Ultra-coarse, single-glance human face detection in a dynamic visual stream. *Neuroimage, 176*, 465–476. https://doi.org/10.1016/j.neuroimage.2018.04.034

Rączy, K., Linke, M., van den Hurk, J., Heitmann, C., Guerreiro, M. J. S., Zhan, M., Kekunnaya, R., Goebel, R., & Röder, B. (2024). Visual and auditory object representations in ventral visual cortex after restoring sight in humans. *bioRxiv, 2024*. https://doi.org/10.1101/2024.11.22.624459, 11.22.624459.

Röder, B., & Kekunnaya, R. (2022). Effects of early visual deprivation. In B. Röder, & R. Kekunnaya (Eds.), *Oxford research encyclopedia of psychology*. Oxford University Press. https://doi.org/10.1093/acrefore/9780190236557.013.839.

Röder, B., Ley, P., Shenoy, B. H., Kekunnaya, R., & Bottari, D. (2013). Sensitive periods for the functional specialization of the neural system for human face processing. *Proceedings of the National Academy of Sciences, 110*(42), 16760–16765. https://doi.org/10.1073/pnas.1309963110

Retter, T. L., Jiang, F., Webster, M. A., & Rossion, B. (2020). All-or-none face categorization in the human brain. *Neuroimage, 213*, Article 116685. https://doi.org/10.1016/j.neuroimage.2020.116685

Retter, T. L., & Rossion, B. (2016). Uncovering the neural magnitude and spatio-temporal dynamics of natural image categorization in a fast visual stream. *Neuropsychologia, 91*, 9–28. https://doi.org/10.1016/j.neuropsychologia.2016.07.028

Retter, T. L., Rossion, B., & Schiltz, C. (2021). Harmonic amplitude summation for frequency-tagging analysis. *Journal of Cognitive Neuroscience, 33*, 11. https://doi.org/10.1162/jocn_a_01763

Robbins, R. A., Nishimura, M., Mondloch, C. J., Lewis, T. L., & Maurer, D. (2010). Deficits in sensitivity to spacing after early visual deprivation in humans: A comparison of human faces, monkey faces, and houses. *Developmental Psychobiology, 52*(8), 775–781. https://doi.org/10.1002/dev.20473

Rossion, B., Jacques, C., & Jonas, J. (2018). Mapping face categorization in the human ventral occipitotemporal cortex with direct neural intracranial recordings. *Annals of the New York Academy of Sciences, 1426*(1), 5–24. https://doi.org/10.1111/nyas.13596

Rossion, B., Torfs, K., Jacques, C., & Liu-Shuang, J. (2015). Fast periodic presentation of natural images reveals a robust face-selective electrophysiological response in the human brain. *Journal of Vision, 15*(1), 18. https://doi.org/10.1167/15.1.18, 18.

Saunders, K. J., Brown, G., & McCulloch, D. L. (1997). Pattern-onset visual evoked potentials: More useful than reversal for patients with nystagmus. *Documenta Ophthalmologica, 94*(3), 265–274. https://doi.org/10.1007/BF02582984

Schulze-Bonsel, K., Feltgen, N., Burau, H., Hansen, L., & Bach, M. (2006). Visual acuities "Hand Motion" and "Counting Fingers" can be quantified with the Freiburg visual acuity test. *Investigative Opthalmology & Visual Science, 47*(3), 1236. https://doi.org/10.1167/iovs.05-0981

Ulrich, R., & Miller, J. (2001). Using the jackknife-based scoring method for measuring LRP onset effects in factorial designs. *Psychophysiology, 38*(5), 816–827. https://doi.org/10.1111/1469-8986.3850816

World Health Organization. (2019). Vision impairment. In C. Gilbert, M. L. Jackson, F. Kyari, K. Naidoo, G. N. Rao, S. Resnikoff, & S. West (Eds.), *World report on vision* (pp. 10–16). World Health Organization. https://apps.who.int/iris/handle/10665/328717.

Yan, X., Liu-Shuang, J., & Rossion, B. (2019). Effect of face-related task on rapid individual face discrimination. *Neuropsychologia, 129*, 236–245. https://doi.org/10.1016/j.neuropsychologia.2019.04.002